Group Theoretical Analysis of non-Newtonian Fluid Flow, Heat and Mass Transfer over a Stretching Surface in the Presence of Thermal Radiation

M. Nazim Tufail[1,3†], A. Saeed Butt[1] and A. Ali[1,2]

[1] *Department of Mathematics, Quaid-e-Azam University, Islamabad 44000, Pakistan*

[2] *Department of Mathematics and Natural Sciences, Prince Muhammad Bin Fahd University 1664, Al Khobar 31952, Saudi Arabia*

[3] *Department of Mathematics, University of Management and Technology Sialkot Campus, Sialkot 51310, Pakistan*

† *Corresponding Author Email*: *nazimtufail@gmail.com*

ABSTRACT

The present article examines the flow, heat and mass transfer of a non-Newtonian fluid known as Casson fluid over a stretching surface in the presence of thermal radiations effects. Lie Group analysis is used to reduce the governing partial differential equations into non-linear ordinary differential equations. These equations are then solved by an analytical technique known as Homotopy Analysis Method (HAM). A comprehensive study of the problem is being made for various parameters involving in the equations through tables and graphs.

Keywords: Lie group analysis; Heat transfer; Magnetic field; Mass transfer; Thermal radiation.

1. INTRODUCTION

The popularity of non-Newtonian fluids has been a dynamic area of research because of its applications. Examples of such fluids include coal-oil slurries, grease, paints, clay coating and suspensions, shampoo, cosmetic products, custard, animals bloods, body fluids and many others. After the initial work done by Crane (1970), a comprehensive and detail research has been made by many scientists and researchers on Newtonian and Non-Newtonian boundary layer flows over stretching surfaces. Gupta and Gupta (1977) studied heat and mass transfer effect over a permeable sheet stretching in its own plane. Grubka and Bobba (1985) used Kummer's function (1965) to study the heat transfer phenomenon along a linearly stretching surface by assuming a power law temperature distribution. Takhar *et al.* (2000) examined the magnetohydrodynamic fluid flow and mass transfer on a stretching surface with chemically reactive species. Mehmood and Ali (2008) analyzed three dimensional viscous flow and heat transfer over a stretching surface. Bhargava *et al.* (2007) used finite element technique

to study the pulsating flow of non-newtonian fluid known as Casson fluid in a non-Darcian porous medium. The unsteady boundary layer flow adjacent to permeable stretching surface in a porous medium was studied by Ali and Mehmood (2008). Flow and heat transfer on a stretching surface in a rotating fluid with a magnetic field analyzed by Takhar (2003). Butt *et al.* (2012) studied the effects of viscoelasticity on entropy generation in a flow through a porous medium over a stretching sheet. Beg *et al.* (2009) analyzed the free convection MHD flow, heat and mass transfer over a stretching surface through a saturated porous medium and also examined the Soret and Dufour effects during the flow phenomenon. A lot of work has been done on Non-Newtonion fluid flows under consideration of different geometries (Tufail *et al.* 2014; Butt *et al.* 2014; Hayat *et al.* 2014; Nadeem *et al.* 2014; Afify *et al.* 2014; Shehzad *et al.* 2014; Haq *et al.* 2015; Hamad *et al.* 2012; Boyd *et al.* 2007; Attia and Ahmed 2010; Khader and Megahed 2013). Arasu *et al.* (2011) used Lie theoretical analysis to study the thermal diffusion effects on free convection flow over a porous stretching sheet with variable

stream conditions. Lie symmetries are useful as they successfully reduce the number of independent variables of the problem. Reviews for the theory and applications of Lie group analysis to differential equations may be found in (Olver 1986 and Bluman and Kumei 1989). Yurusoy and Pakdemirli (1999) used group theoretical analysis to obtain the exact solution of second grade fluid over a stretching surface. Afify (2009) made use of Lie symmetries to study MHD(magnetohydrodynamics) aligned creeping flow and heat transfer in second grade fluids. Later, Mehmood *et al.* (2005) used symmetry reduction to examine unsteady MHD aligned second grade flow and found the general solution. The aim of this article is to analyze flow, heat and mass transfer of Non-Newtonian fluid known as Casson fluid over a stretching surface embedded in a porous medium in the presence of a uniform magnetic field and thermal radiation effects. Lie group analysis is used to reduce the governing equations into non-linear ordinary differential equations. These equations are then solved using Homotopy Analysis Method (HAM) and a complete analysis of the problem is presented. The effects of various physical parameters governing the equations are discussed and interpreted through tables and graphs.

2. MATHEMATICAL FORMULATION OF THE PROBLEM

Consider a steady, two-dimensional laminar flow of an incompressible Casson fluid over a stretching surface through a porous medium. The sheet lies in the plane $\bar{y} = 0$ with the flow being confined to $\bar{y} > 0$. The coordinate $\bar{x}$ is being taken along the stretching surface and $\bar{y}$ is normal to the surface. Along the $\bar{x}$-axis, two equal and opposite forces are applied, so that the surface is stretched, keeping the origin fixed. A uniform transverse magnetic field of strength B_0 is applied parallel to $\bar{y}$-axis. It is also assumed that the fluid is electrically conducting and the magnetic Reynolds number is small so that the induced magnetic field is neglected. No electric field is assumed to exist. By following Nakamura and Sawada (1988) we use the biviscosity modified Casson rheological model. The rheological equation of state for an isotropic and incompressible flow of a Casson fluid is

$$\tau_{ij} = \begin{cases} 2(\mu_B + \frac{p_y}{\sqrt{2\pi}})e_{ij}, \pi > \pi_c \\ 2(\mu_B + \frac{p_y}{\sqrt{2\pi_c}})e_{ij}, \pi < \pi_c \end{cases} \tag{1}$$

Here $\pi = e_{ij}e_{ij}$ is the product of the component of deformation rate with itself, e_{ij} is the $(i, j)th$ component of the deformation rate, π_c

is a critical value of this product based on the non-Newtonian model, μ_B is plastic dynamic viscosity of the non-Newtonian fluid and p_y is the yield stress of fluid. Using (1) and conservation of mass, momentum, heat transfer and mass transfer, the following boundary layer equations are obtained

$$\frac{\partial \bar{u}}{\partial \bar{x}} + \frac{\partial \bar{v}}{\partial \bar{y}} = 0, \tag{2}$$

$$\bar{u}\frac{\partial \bar{u}}{\partial \bar{x}} + \bar{v}\frac{\partial \bar{u}}{\partial \bar{y}} = \frac{\mu}{\rho}(1 + \frac{1}{\beta})\frac{\partial^2 \bar{u}}{\partial \bar{y}^2} - \frac{\upsilon}{k'}\bar{u} - \frac{\sigma B_0^2}{\rho}\bar{u}, \tag{3}$$

$$\bar{u}\frac{\partial T}{\partial \bar{x}} + \bar{v}\frac{\partial T}{\partial \bar{y}} = \frac{k}{\rho c_p}\frac{\partial^2 T}{\partial \bar{y}^2} + \frac{16\sigma_1 T_\infty^3}{3\rho c_p k_1}\frac{\partial^2 T}{\partial \bar{y}^2}, \tag{4}$$

$$\bar{u}\frac{\partial C}{\partial \bar{x}} + \bar{v}\frac{\partial C}{\partial \bar{y}} = D\frac{\partial^2 C}{\partial \bar{y}^2}, \tag{5}$$

The boundary conditions for the momentum and energy equation are [11];

$$\begin{aligned} \bar{u}(\bar{x},\bar{y}) &= b\bar{x}, \bar{v}(\bar{x},\bar{y}) = 0 \text{ at } \bar{y} = 0, \\ \bar{u}(\bar{x},\bar{y}) &= 0, \text{ at } \bar{y} \to \infty. \end{aligned} \tag{6}$$

$$\begin{aligned} T(\bar{x},\bar{y}) &= T_w, C(\bar{x},\bar{y}) = C_w \text{ at } \bar{y} = 0, \\ T(\bar{x},\bar{y}) &= T_\infty, C(\bar{x},\bar{y}) = C_\infty, \text{ at } \bar{y} \to \infty. \end{aligned} \tag{7}$$

where μ is the constant viscosity, ρ is fluid density, $\nu = \frac{\mu}{\rho}$, is kinematic viscosity, $\beta = \frac{\mu_B\sqrt{2\pi_c}}{p_y}$ is Casson fluid parameter, σ is electrical conductivity of fluid, k' is permeability of medium, c_p is specific heat at constant pressure, k is thermal conductivity of the fluid, D is mass diffusivity, T and T_∞ are fluid and ambient temperatures respectively, T_w is wall temperature, C is concentration of fluid, C_w is species concentration at the surface, C_∞ is free stream concentration of the species, $\bar{u}, \bar{v}$ are velocity components in $\bar{x}$- and $\bar{y}$- directions and b is stretching parameter. Introducing the following similarity transformations

$$\begin{aligned} u(x,y) &= \frac{\bar{u}(\bar{x},\bar{y})}{\sqrt{b\upsilon}}, v(x,y) = \frac{\bar{v}(\bar{x},\bar{y})}{\sqrt{b\upsilon}}, \\ \theta(x,y) &= \frac{T(\bar{x},\bar{y}) - T_\infty}{(T_w - T_\infty)}, x = \sqrt{\frac{b}{\nu}}\bar{x}, \end{aligned} \tag{8}$$

$$\phi(x,y) = \frac{C(\bar{x},\bar{y}) - C_\infty}{(C_w - C_\infty)}, y = \sqrt{\frac{b}{\nu}}\bar{y}. \tag{9}$$

Using the transformations $(8 - 9)$ in Eqs. $(2 - 7)$, we have

$$\frac{\partial u}{\partial x} + \frac{\partial v}{\partial y} = 0, \tag{10}$$

$$u\frac{\partial u}{\partial x} + v\frac{\partial u}{\partial y} = (1 + \frac{1}{\beta})\frac{\partial^2 u}{\partial y^2} - \frac{1}{K}u - Mu, \quad (11)$$

$$u\frac{\partial \theta}{\partial x} + v\frac{\partial \theta}{\partial y} = \frac{1}{Pr}(1 + \frac{4}{3Nr})\frac{\partial^2 \theta}{\partial y^2}, \quad (12)$$

$$u\frac{\partial \phi}{\partial x} + v\frac{\partial \phi}{\partial y} = \frac{1}{Sc}\frac{\partial^2 \phi}{\partial y^2}. \quad (13)$$

$$au(x,y) = x, \; v(x,y) = 0 \; \text{ at } y = 0,$$

$$u(x,y) = 0, \; \text{ at } y \to \infty. \quad (14)$$

$$\theta(x,y) = 1, \; \phi(x,y) = 1 \; \text{ at } y = 0$$

$$\theta(x,y) = 0, \; \phi(x,y) = 0 \; \text{ at } y \to \infty. \quad (15)$$

where $K = \frac{k'b}{v}$ is permeability parameter, $M = \frac{\sigma B_0^2}{\rho b}$ is magnetic field parameter, $Pr = \frac{\mu c_p}{\kappa}$ is Prandtl number, $Nr = \frac{\kappa \kappa_1}{4\sigma_1 T_\infty^3}$ is radiation parameter and $Sc = \frac{v}{b}$ is Schmidt number. Now by introducing stream function

$$u = \frac{\partial \psi}{\partial y}, \text{ and } v = -\frac{\partial \psi}{\partial x}. \quad (16)$$

Eq.(10) will become identically zero and the system (11-15) takes the form

$$\psi_y\psi_{xy} - \psi_x\psi_{yy} + M\psi_y + \frac{1}{K}\psi_y - (1 + \frac{1}{\beta})\psi_{yyy} = 0, (17)$$

$$\psi_y\theta_x - \psi_x\theta_y - \frac{1}{Pr}(1 + \frac{4}{3Nr})\theta_{yy} = 0, \quad (18)$$

$$\psi_y\phi_x - \psi_x\phi_y - \frac{1}{Sc}\phi_{yy} = 0. \quad (19)$$

$$\frac{\partial \psi(x,0)}{\partial y} = x, \frac{\partial \psi(x,0)}{\partial x} = 0, \frac{\partial \psi(x,\infty)}{\partial y} = 0 \quad (20)$$

$$\theta(x,y) = 1, \; \phi(x,y) = 1 \; \text{ at } y = 0 \quad (21)$$

$$\theta(x,y) = 0, \; \phi(x,y) = 0 \; \text{ at } y \to \infty \quad (22)$$

3. LIE GROUP ANALYSIS

A symmetry of a differential equation is an inevitable transformation of the dependent and independent variables that maps the equation to itself. Amongst symmetries of differential equations, those depending continuously on a small parameter and forming a local one-parameter

group of transformation can be calculated algorithmically through a procedure due to Sophus Lie (1875). One of the most useful and striking properties of symmetries is that they map solutions to solutions. For partial differentials, symmetries allow the reduction of the number of independent variables. Consider the one-parameter Lie group of infinitesimal transformations in (x,y,ψ,θ,ϕ) given by

$$\begin{aligned} x^* &= x + \varepsilon\xi(x,y,\psi,\theta,\phi) + O(\varepsilon^2), \\ y^* &= y + \varepsilon\tau(x,y,\psi,\theta,\phi) + O(\varepsilon^2), \\ \psi^* &= \psi + \varepsilon\Gamma(x,y,\psi,\theta,\phi) + O(\varepsilon^2), \\ \theta^* &= \theta + \varepsilon\Omega(x,y,\psi,\theta,\phi) + O(\varepsilon^2), \\ \phi^* &= \phi + \varepsilon\Phi(x,y,\psi,\theta,\phi) + O(\varepsilon^2), \quad (23) \end{aligned}$$

where ε is the Lie group parameter. Equations $(17-19)$ are nonlinear partial differential equation with three dependent variables (ψ,θ,ϕ) and two independent variables (x,y). Lie group analysis is required so that Eqs. $(17-19)$ remain invariants under these transformations which yields an over-determined, linear system of equations for infinitesimals $\xi, \tau, \Gamma, \Omega, \Phi$. The symmetry group infinitesimal generator is defined by

$$\begin{aligned} \vec{V} &= \xi(x,y,\psi,\theta,\phi)\frac{\partial}{\partial x} + \tau(x,y,\psi,\theta,\phi)\frac{\partial}{\partial y} \\ &+ \Gamma(x,y,\psi,\theta,\phi)\frac{\partial}{\partial \Psi} + \Omega(x,y,\psi,\theta,\phi)\frac{\partial}{\partial \theta} \\ &+ \Phi(x,y,\psi,\theta,\phi)\frac{\partial}{\partial \phi}, \quad (24) \end{aligned}$$

After following the procedure defined in (Olver 1989) to calculate the infinitesimals we have

$$\begin{aligned} \xi &= c_1 + c_2 x, \; \tau = f_1(x), \\ \Gamma &= c_3 + c_2\psi, \Omega = c_4 + c_5\theta, \\ \Phi &= c_6 + c_7\phi. \quad (25) \end{aligned}$$

where $c_i(i = 1,2,...,7)$, are arbitrary constants and $f_1(x)$ is arbitrary function of x. After fixing the constants as $c_1 = c_3 = c_4 = c_5 = c_6 = c_7 = f_1(x) = 0, c_2 = 1$ we get

$$\frac{dx}{x} = \frac{dy}{0} = \frac{d\psi}{\psi} = \frac{d\theta}{0} = \frac{d\phi}{0}, \quad (26)$$

$$y = \eta, \; \psi = xf(\eta), \; \theta = \theta(\eta), \; \phi = \phi(\eta). \quad (27)$$

Here f, θ and ϕ are the functions of η. After using above transformations the system $(17 - 22)$ becomes

$$(1+\frac{1}{\beta})f'''(\eta)+f(\eta)f''(\eta)-f'(\eta)^2$$

$$-(M+\frac{1}{K})f'(\eta)=0, \qquad (28)$$

$$(1+\frac{4}{3Nr})\theta''(\eta)+Pr\,f(\eta)\theta'(\eta)=0, \qquad (29)$$

$$\phi''(\eta)+Scf(\eta)\phi'(\eta)=0. \qquad (30)$$

$$f(0)=0, f'(0)=1, f'(\infty)=0, \qquad (31)$$

$$\theta(0)=1, \theta(\infty)=0, \phi(0)=1, \phi(\infty)=0. \qquad (32)$$

The skin friction coefficient, the local Nusselt number and the local Sherwood number are defined as:

$$
\begin{aligned}
C_f &= \frac{\left(\mu_B+\frac{p_y}{\sqrt{2\pi_c}}\right)}{\rho(b\bar{x})^2}\left(\frac{\partial \bar{u}}{\partial \bar{y}}\right)_{y=0}, \\
Nu_x &= \frac{\bar{x}}{(T_w-T_\infty)}\left(\frac{\partial T}{\partial \bar{y}}\right)_{y=0}, \\
Sh_x &= \frac{\bar{x}}{(C_w-C_\infty)}\left(\frac{\partial C}{\partial \bar{y}}\right)_{y=0}. \qquad (33)
\end{aligned}
$$

Using $(8-9)$ and (33), the dimensionless form of skin friction, local Nusselt number and local Sherwood number become

$$
\begin{aligned}
Re_x^{1/2}C_f &= -(1+\frac{1}{\beta})f''(0), \\
Re_x^{-1/2}Nu_x &= -\theta'(0), \\
Re_x^{-1/2}Sh_x &= -\phi'(0). \qquad (34)
\end{aligned}
$$

4. SOLUTION OF THE PROBLEM

In order to solve the non-linear Eqs. $(28-30)$ with boundary conditions $(31-32)$, an analytical technique known as Homotopy Analysis Method (HAM) is used. According to the nature of the problem, following set of initial guesses and auxiliary linear operators for $f(\eta)$, $\theta(\eta)$ and $\phi(\eta)$ are used:

$$
\begin{aligned}
f_0(\eta) &= 1-\exp(-\eta), \theta_0(\eta)=\exp(-\eta), \\
\phi_0(\eta) &= \exp(-\eta), \qquad (35)
\end{aligned}
$$

$$
\begin{aligned}
\mathcal{L}_f &= \frac{d^3 f}{d\eta^3}-\frac{df}{d\eta}, \mathcal{L}_\theta=\frac{d^2\theta}{d\eta^2}+\frac{d\theta}{d\eta}, \\
\mathcal{L}_\phi &= \frac{d^2\phi}{d\eta^2}+\frac{d\phi}{d\eta}, \qquad (36)
\end{aligned}
$$

The zero-order deformation equations and boundary conditions are:

$$(1-p)\mathcal{L}_f[\hat{f}(\eta;p)-f_0(\eta)]=p\hbar_f\mathcal{N}_f\left[\hat{f}(\eta;p)\right],$$

$$(1-p)\mathcal{L}_\theta[\hat{\theta}(\eta;p)-\theta_0(\eta)]=p\hbar_\theta\mathcal{N}_\theta\left[\hat{f}(\eta;p),\hat{\theta}(\eta;p)\right],$$

$$(1-p)\mathcal{L}_\phi[\hat{\phi}(\eta;p)-\phi_0(\eta)]=p\hbar_\phi\mathcal{N}_\phi\left[\hat{f}(\eta;p),\hat{\phi}(\eta;p)\right].$$

$$
\begin{aligned}
\hat{f}(0;p) &= 0, \hat{f}'(0;p)=1, \\
\hat{f}'(\infty;p) &= 0, \\
\hat{\theta}(0;p) &= 1, \hat{\theta}(\infty;p)=0, \\
\hat{\phi}(0;p) &= 1, \hat{\phi}(\infty;p)=0. \qquad (37)
\end{aligned}
$$

where $\hbar_f$, $\hbar_\theta$ and $\hbar_\phi$ indicates the non-zero auxiliary parameters and $p \in [0,1]$ is the embedding parameter. The non-linear operators are

$$\mathcal{N}_f\left[\hat{f}(\eta;p)\right]=(1+\frac{1}{\beta})\frac{\partial^3\hat{f}(\eta;p)}{\partial\eta^3}$$

$$+\hat{f}(\eta;p)\frac{\partial^2\hat{f}(\eta;p)}{\partial\eta^2}-(\frac{\partial\hat{f}(\eta;p)}{\partial\eta})^2$$

$$-(M+\frac{1}{K})\frac{\partial\hat{f}(\eta;p)}{\partial\eta},$$

$$\mathcal{N}_\theta\left[\hat{\theta}(\eta;p),\hat{f}(\eta;p)\right]=(1+\frac{4}{3Nr})\frac{\partial^2\hat{\theta}(\eta;p)}{\partial\eta^2}$$

$$+Pr\,\hat{f}(\eta;p)\frac{\partial\hat{\theta}(\eta;p)}{\partial\eta},$$

$$\mathcal{N}_\phi\left[\hat{\phi}(\eta;p),\hat{f}(\eta;p)\right]=\frac{\partial^2\hat{\phi}(\eta;p)}{\partial\eta^2}$$

$$+Sc\,\hat{f}(\eta;p)\frac{\partial\hat{\phi}(\eta;p)}{\partial\eta}.$$

The mth-order deformation equations are given as

$$
\begin{aligned}
\mathcal{L}_f\left[f_m(\eta)-\chi_m f_{m-1}(\eta)\right] &= \hbar_f\mathcal{R}_m^f(\eta), &(37) \\
\mathcal{L}_\theta\left[\theta_m(\eta)-\chi_m\theta_{m-1}(\eta)\right] &= \hbar_\theta\mathcal{R}_m^\theta(\eta), &(38) \\
\mathcal{L}_\phi\left[\phi_m(\eta)-\chi_m\phi_{m-1}(\eta)\right] &= \hbar_\phi\mathcal{R}_m^\phi(\eta), &(39)
\end{aligned}
$$

where

$$\mathcal{R}_m^f(\eta)=\frac{\partial^3 f_{m-1}}{\partial\eta^3}-(M+\frac{1}{K})\frac{\partial f_{m-1}}{\partial\eta}$$

$$+ \sum_{k=0}^{m-1} \left(f_{m-1-k} \frac{\partial^2 f_k}{\partial \eta^2} - \frac{\partial f_{m-1-k}}{\partial \eta} \frac{\partial f_k}{\partial \eta} \right),$$

$$\mathcal{R}_m^{\theta}(\eta) = (1 + \frac{4}{3Nr}) \frac{\partial^2 \theta_{m-1}}{\partial \eta^2} + \Pr \sum_{k=0}^{m-1} f_{m-1-k} \frac{\partial \theta_k}{\partial \eta},$$

$$\mathcal{R}_m^{\phi}(\eta) = \frac{\partial^2 \phi_{m-1}}{\partial \eta^2} + Sc \sum_{k=0}^{m-1} f_{m-1-k} \frac{\partial \phi_k}{\partial \eta}.$$

Here

$$\chi_m = \begin{cases} 0, & m \le 1, \\ 1, & m > 1. \end{cases} \tag{40}$$

The series solutions obtained by HAM for Eqs. $(28 - 30)$ subject to boundary conditions $(31 - 32)$ can be written as:

$$f(\eta) = \sum_{m=0}^{\infty} f_m(\eta), \quad \theta(\eta) = \sum_{m=0}^{\infty} \theta_m(\eta), \tag{41}$$

$$\phi(\eta) = \sum_{m=0}^{\infty} \phi_m(\eta). \tag{42}$$

4.1 Convergence of the solutions

It is observed that the series solutions $(41 - 42)$ contains the auxiliary parameters $\hbar_f, \hbar_{\theta}$ and $\hbar_{\phi}$ with the help of which the convergence region and rate of approximation of series solutions can be controlled and adjusted. To get an idea of the admissible ranges of $\hbar_f, \hbar_{\theta}$ and $\hbar_{\phi}$ in which the series solution converge, the so-called $\hbar$-curves are plotted at the $20th$ order of approximation. The range for the admissible values of $\hbar_f, \hbar_{\theta}$ and $\hbar_{\phi}$ are $-0.5 < \hbar_f < -0.1$, $-0.5 < \hbar_{\theta} < -0.2$ and $-0.5 < \hbar_{\phi} < -0.1$ as shown in figure 1. To accelerate the convergence of the series solutions (51), the homotopy-Pade approximation is utilized, and the tabulated results for $f''(0)$, $\theta'(0)$ and $\phi'(0)$ at $\hbar_f = -0.35$, $\hbar_{\theta} = -0.35 \hbar_{\phi} = -0.45$ are presented in table 1. It is quite evident that the value of $f''(0)$ converge up to 6 decimal places after 6th order of approximation and the values of $\theta'(0)$ and $\phi'(0)$ are convergent after $8th$ order of approximation.

5. RESULTS AND DISCUSSIONS

In this section, the effects of various parameters on velocity, temperature, and concentration fields are presented through graphs and tables. Figures $1 - 3$ depicts the effects of various parameters on velocity profile. In figure 2, the effects of Casson fluid parameter β on velocity
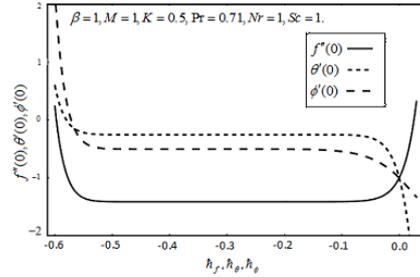
Fig. 1. The $\hbar$-curves of at 20th-order of approximations.

Table 1 Convergence table for the $[m/m]$ homotopy Pade approximation of $f''(0)$, $\theta'(0)$ and $\phi(0)$ when $\beta = 1.0, M = 1.0$, $K = 0.5, Pr = 1.0, Nr = 1.0$ and $Sc = 1.0$ are kept fixed

Pade' Approx.	$-f''(0)$	$-\theta'(0)$	$-\phi'(0)$
$[2,2]$	1.413790	0.252893	0.493297
$[4,4]$	1.414210	0.25365	0.501131
$[6,6]$	1.414210	0.253648	0.501254
$[8,8]$	1.414210	0.253648	0.501250
$[10,10]$	1.414210	0.253648	0.501250

profile are illustrated. It is quite clear that a decrease in velocity occurs with increase in Casson fluid parameter. Figure 3 shows the influence of magnetic field parameter M on velocity profile $f\prime(\eta)$. It is observed that with an increase in the value of M, the velocity decreases. This is due to the reason that the application of magnetic field to an electrically conducting fluid gives rise to resistive force known as Lorentz force which causes the fluid to decelerate. Figure 4 depicts that velocity increases on increasing K because as the permeability parameter increases, a decrease in the resistance of porous medium is observed which speeds up the flow.
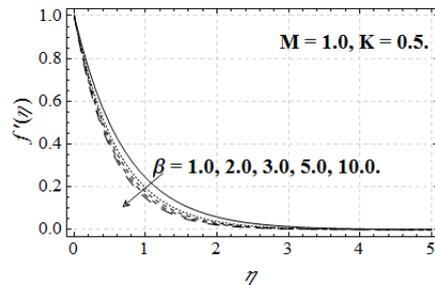
Fig. 2. Effects of β on $f\prime(\eta)$.

The effects of various physical parameters on temperature profile $\theta(\eta)$ are presented in figures $5 - 8$. Figure 5 illustrates that the thermal boundary layer thickness increases with increase in Casson fluid parameter β. The effects
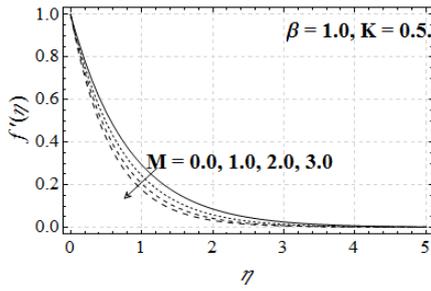
Fig. 3. Effects of M on $f'(\eta)$.
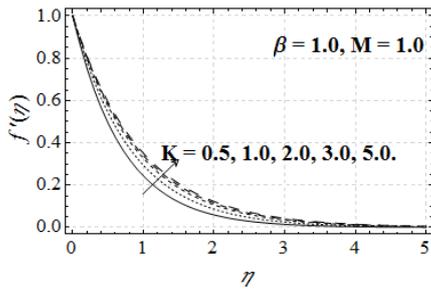
Fig. 4. Effects of K on $f'(\eta)$.

Fig. 5. Effects of β on $\theta(\eta)$.

Fig. 6. Effects of M on $\theta(\eta)$.

Fig. 7. Effects of K on $\theta(\eta)$.
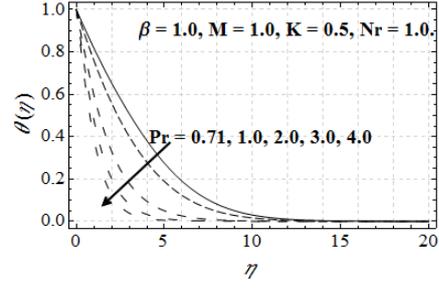
Fig. 8. Effects of Pr on $\theta(\eta)$.
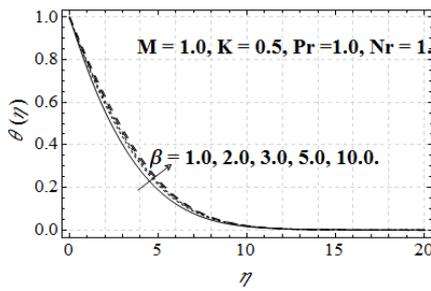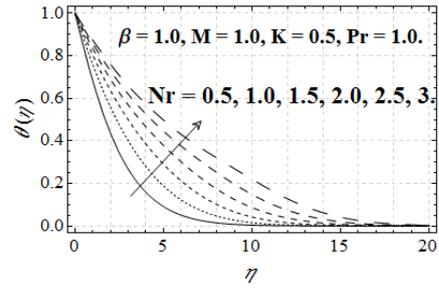
Fig. 9. Effects of Nr on $\theta(\eta)$.
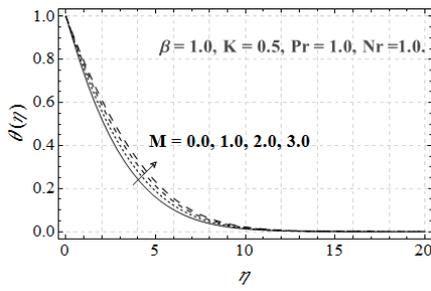
Fig. 10. Effects of β on $\phi(\eta)$.
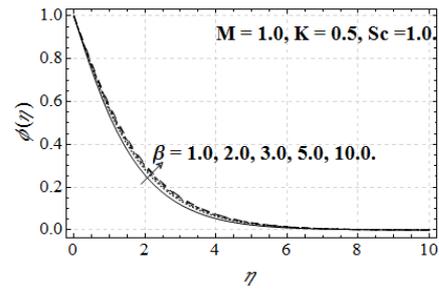
of magnetic field parameter M on temperature profile are increasing as shown in figure 6. The influence of permeability parameter K on $\theta(\eta)$ is depicted in figure 7. A decrease in temperature profile is noticed with increase in permeability parameter. Figure 8 illustrates that thermal boundary layer thickness decreases with increase in Prandtl number Pr. On the other hand, figure 9 demonstrates that thermal radiation parameter Nr enhances fluid temperature.

In figure 10, the influence of Casson fluid parameter β on concentration profile $\phi(\eta)$ are shown. An increase in concentration profile is observed with increase in β. The concentration boundary layer increases with magnetic field parameter M and decreases with permeability parameter K and Schmidt number Sc as shown in figures 11, 12 and 13 respectively.
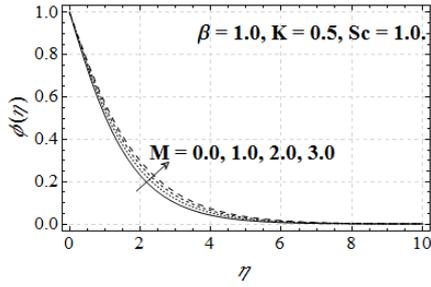
Fig. 11. Effects of M on $\phi(\eta)$.
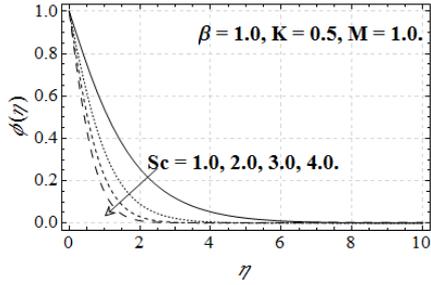
Fig. 12. Effects of Sc on $\phi(\eta)$.
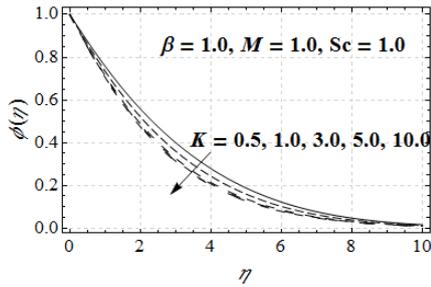
Fig. 13. Effects of K on $\phi(\eta)$.

In order to validate our findings, we have tabulated a comparison of values of $-f''(0)$ with those reported earlier [18] presented in Table 2. By keeping $\beta = \infty$ and $K = \infty$, we have found that the values obtained in this study are in good agreement with those reported earlier [18].

Table 2 A comparison of $-f''(0)$ obtained by the analytical method with the Cortell studies [18] when we fixed $K = \infty$ & $\beta = \infty$

M	$-f''(0)$ Present	$-f''(0)$ [18]
0.0	1.00000	1.00000
0.2	1.09549	1.09545
0.5	1.22476	1.22475
1.0	1.41421	1.41421
1.2	1.48324	1.48324
1.5	1.58114	1.58114
2.0	1.732051	1.73205

Table 3 Effects of various parameters on $-\left(1 + \frac{1}{\beta}\right) f''(0)$ when $h_f = 0.35$

β	M	K	$-\left(1+\frac{1}{\beta}\right) f''(0)$
0.5	1.0	0.5	3.46410
1.0			2.82843
1.5			2.58199
2.0			2.44949
0.5	0.5	0.5	3.24037
	1.0		3.46410
	1.5		3.67423
	2.0		3.87298
0.5	1.0	0.5	3.46410
		1.0	3.00000
		1.5	2.82843
		2.0	2.73861

Table 4 Effects of various parameters on $-\theta'(0)$ when $h_f = 0.35, h_\theta = 0.45$

β	M	K	Pr	Nr	$-\theta'(0)$
0.5	1.0	0.5	0.71	1.0	0.218459
1.0					0.188432
1.5					0.175448
2.0					0.168150
0.5	0.5	0.5	0.71	1.0	0.228523
	1.0				0.218459
	1.5				0.209624
	2.0				0.201784
0.5	1.0	0.5	0.71	1.0	0.218459
		1.0			0.240133
		1.5			0.248948
		2.0			0.253742
0.5	1.0	0.5	0.71	1.0	0.218459
			1.0		0.289864
			2.0		0.492932
			3.0		0.655593
0.5	1.0	0.5	0.71	0.5	0.288460
				1.0	0.218459
				1.5	0.176120
				2.0	0.147643

Table 3 presents the values of $-\left(1 + \frac{1}{\beta}\right)f''(0)$ for various values of Casson fluid parameter β, Magnetic field parameter M and permeability parameter K. The skin friction coefficient decreases with β and K and increases with M. Table 4 shows that the local Nusselt number $-\theta'(0)$ increases with permeability parameter K and Prandtl number Pr and decreases with Casson fluid parameter β, magnetic field parameter M and radiation parameter Nr. In Table 5 demonstrates the effects of pertinent parameters on local Sherwood number. It is seen that $-\phi'(0)$ augments with permeability parameter and Schmidt number Sc and decreases with Cas-

Table 5 Effects of various parameters on $-\phi'(0)$ **when** $h_f = 0.35, h_\phi = 0.45$

β	M	K	Sc	$-\phi'(0)$
0.5	1.0	0.5	0.71	0.429091
1.0				0.384405
1.5				0.363575
2.0				0.351450
0.5	0.5	0.5	0.71	0.443042
	1.0			0.429092
	1.5			0.416431
	2.0			0.404862
0.5	0.5	0.5	0.71	0.429092
		1.0		0.458545
		1.5		0.469915
		2.0		0.475961
0.5	0.5	0.5	0.71	0.429092
			1.0	0.550535
			2.0	0.877907
			3.0	1.13143

son fluid parameter β, magnetic field parameter *M*.

6. CONCLUSIONS

The boundary layer flow of a magnetohydrodynamic, Casson fluid in a porous medium over a stretching surface is studied. The symmetries of the partial differential equations are found and translational symmetries are used to reduce the equations to non-linear ordinary differential equations. Homotopy Analysis method is used to solve the equations. Following observations are found from the study:

• A decrease in momentum boundary layer thickness is observed with increase in Casson fluid parameter β and magnetic field parameter *M*.

• An increase in fluid velocity is noticed with increase in permeability parameter *K*.

• The thermal boundary layer thickness increases with Casson fluid parameter β, magnetic field parameter *M* and radiation parameter *Nr*.

• A decreasing effect is noticed on temperature is noticed with increase in permeability parameter *K* and Prandtl number *Pr*.

• The concentration increases with Casson fluid parameter β and magnetic field parameter *M* and decreases with permeability parameter *K* and Schmidt number *Sc*.

• Skin friction increases with magnetic field parameter *M* and decreases with Casson fluid parameter β and permeability parameter *K*.

• The permeability parameter *K* and Prandtl number *Pr* has increasing effects on local Nusselt number and it decreases with Casson fluid parameter β, magnetic field parameter *M* and radiation parameter *Nr*.

• Local Sherwood number increase with *M* and *Sc* and decrease with β and *M*.

REFERENCES

Abramowitz, M., I. A. Stegun (1965). *Handbook of Mathematical functions.* (USA: National Bureau of Standards, Washington).

Afify, A. A., M. J. Uddin and M. Ferdows (2014). Scaling group transformation for MHD boundary layer flow over permeable stretching sheet in presence of slip flow with Newtonian heating effects. *Appl. Math. Mech.-Eng. 35*, 1375-1386.

Afify, A. A. (2009). Some new exact solutions for MHD aligned creeping flow and heat transfer in second grade fluids by using Lie group analysis. *Nonlinear Analysis 70*, 3298-3306.

Arasu, P. P., P. Loganathana, R. Kandasamy and I. Muhaimin (2011). Lie group analysis for thermal-diffusion and diffusion-thermo effects on free convective flow over a porous stretching surface with variable stream conditions in the presence of thermophoresis particle deposition. *Nonlin. Anal., Hybrid Systems 5,* 20-31.

Ali, A. and A. Mehmood (2008). Homotopy analysis of unsteady boundary layer flow adjacent to perrmeable stretching surface in a porous medium. *Commu. Nonlinear Sci. Numer. Simul. 13* (2) 340-349.

Attia, H. A. and M. E. S. Ahmed (2010). Transient MHD Couette flow of a Casson fluid between parallel plates with heat transfer. Italian *J.PureAppl.Math. 27*, 19-38.

Bég, O. A., A. Y. Bakier and V. R. Prasad, (2009). Numerical study of free convection magnetohydrodynamic heat and mass transfer from a stretching surface to a saturated porous medium with Soret and Dufour effects. *Computational Materials Science 46*, 57-65.

Bhargava, R., H. S. Takhar, S. Rawat, T. A. Bég and O. A. Bég (2007). Finite Element Solutions For Non-

Newtonian Pulsatile Flow in a *Non-Darcian Porous Medium Conduit. Non.Lin. Analysis 12*(3), 317-327.

Butt, A. S., S. Munawar, A. Mehmood and A. Ali (2012). Effect of viscoelasticity on entropy generation in a porous medium over a stretching plate. *World Appl. Sci. J. 17* (4), 516-523.

Butt, A. S., M. N. Tufail and A. Ali (2014). Three dimensional flow of magnetohydrodynamic Casson fluid over an unsteady stretching sheet embedded in a porous medium. *J.Appl. Mech.Tech. Phy.* (Accepted).

Bluman, G. W. and S. Kumei (1989). *Symmetries and Differential Equations.* Springer, New York.

Boyd, J., J. M. Buick and S. Green (2007). Analysis of the Casson and Carreau-Yasuda Non-Newtonian blood models in steady and oscillatory flow using the Lattice Boltzmann Method. *Phys. Fluids 19,* 93-103.

Crane, L. J. (1970). Flow past a stretching sheet. *Zeitschrift für angewandte Mathematik und Physik 21,* 645-647.

Gupta, P. S. and A. S. Gupta (1977). Heat and Mass Transfer on a stretching sheet with suction or blowing. *Can. J. of Chem. Eng.* 55 744-746.

Grubka, J. and K. M. Bobba (1985). Heat transfer characteristics of a continuous stretching surface with variable temperature. ASME, J. Heat Trans. 107, 248-250.

Hayat, T., F. M. Abbasi and A. Alsaedi (2014). Soret and Dufour Effects on Peristaltic Flow in an Asymmetric Channel. *Arab. J. Sci. Eng., 39,* 4341-4349.

Haq, R., S. Nadeem, Z. H. Khan and N. S. Akbar (2015). Thermal radiation and slip effects on MHD stagnation point flow of nanofluid over a stretching sheet. *Physica E. 65,* 17-23.

Hamad, M. A. A., M. J. Uddin and A. I. M. Ismail (2012). Radiation effects on heat and mass transfer in MHD stagnation-point flow over a permeable flat plate with thermal convective surface boundary condition, temperature dependent viscosity and thermal conductivity. *Nuclear Eng. Design 242,* 194-200.

Khader, M. M. and A. M. Megahed (2013). Numerical studies for flow and heat transfer of the Powell-Eyring fluid thin film over an unsteady stretching sheet with internal heat generation using the ehebyshev finite difference method. *JAMT 54*(3), 440-450.

Lie, S. (1875). Zur Theorie des Integrabilitatsfaktors, *Christ, Forh., Aar 1874,* 242-254.

Mehmood, A. and A. Ali (2005). Symmetry Reduction of Unsteady MHD aligned second grade Flow Equations. *Math. Comp. Appl. 10* (3), 395-402.

Mehmood, A. and A. Ali (2008). Analytic solution of three-dimensional viscous flow and heat transfer over a stretching flat surface by homotopy analysis method. *ASME-J. Heat Trans. 130 ,* 121701-121707.

Nadeem, S., R. Mehmood and N. S. Akbarb (2014). Optimized analytical solution for oblique flow of a Casson-nano fluid with convective boundary conditions. *Int. J. Therm. Sci. 78,* 90-100.

Nakamura, M., Sawada, T. (1988). Numerical study on the flow of a non-Newtonian fluid through an axisymmetric stenosis. *ASME J. Biomech. Eng.* 110-137.

Olver, P. J. (1986). *Applications of Lie Groups to Differential Equations.* (Springer Verlag).

Shehzad, S. A., T. Hayat, A. Alsaedi and M. A. Obid (2014). Nonlinear thermal radiation in three-dimensional flow of Jeffrey fluid: A model for solar energy. *Appl. Math. and Comp. 248,* 273-286.

Takhar, H. S., A. J. Chamkha and G. Nath (2000). Flow and mass transfer on a stretching sheet with a magnetic field and chemically reactive species. *Int. J. Eng. Sci. 38,* 1303-1314.

Takhar, H. S., A. J. Chamkha and G. Nath (2003). Flow and heat transfer on a stretching surface in a rotating fluid with a magnetic field. *Int. J. Therm. Sci. 42,* 23-31.

Tufail, M. N., A. S. Butt and A. Ali (2014). Heat source/sink effects on Non-Newtonian MHD fluid flow and heat transfer over a permeable stretching surface. Lie group analysis. *Indian J. Phys. 80,* 75-82.

Yurusoy, M. and M. Pakdemirli (1999). Exact solutions of boundary layer equations of a special non-Newtonian fluid over a stretching sheet. *Mech. Res. Commun. 26,* 171-175.